



HAL
open science

Stress-induced large Curie temperature enhancement in Fe₆₄Ni₃₆ Invar alloy

Pedro Gorria, David Martínez-Blanco, Maria J. Perez, Jesús A. Blanco,
Antonio Hernando, María A. Laguna-Marco, Daniel Haskel, Narcizo M.
Souza-Neto, Ronald I. Smith, W.G. Marshall, et al.

► **To cite this version:**

Pedro Gorria, David Martínez-Blanco, Maria J. Perez, Jesús A. Blanco, Antonio Hernando, et al.. Stress-induced large Curie temperature enhancement in Fe₆₄Ni₃₆ Invar alloy. *Physical Review B: Condensed Matter and Materials Physics* (1998-2015), 2009, 80 (6), pp.064421. 10.1103/PhysRevB.80.064421 . insu-00498748

HAL Id: insu-00498748

<https://insu.hal.science/insu-00498748>

Submitted on 11 Mar 2022

HAL is a multi-disciplinary open access archive for the deposit and dissemination of scientific research documents, whether they are published or not. The documents may come from teaching and research institutions in France or abroad, or from public or private research centers.

L'archive ouverte pluridisciplinaire **HAL**, est destinée au dépôt et à la diffusion de documents scientifiques de niveau recherche, publiés ou non, émanant des établissements d'enseignement et de recherche français ou étrangers, des laboratoires publics ou privés.



Distributed under a Creative Commons Attribution 4.0 International License

Stress-induced large Curie temperature enhancement in Fe₆₄Ni₃₆ Invar alloy

Pedro Gorria, David Martínez-Blanco, María J. Pérez, and Jesús A. Blanco
Departamento de Física, Universidad de Oviedo, Calvo Sotelo, s/n, 33007 Oviedo, Spain

Antonio Hernando
Instituto de Magnetismo Aplicado, UCM-ADIF-CSIC, P.O. Box 155, Las Rozas, 28230 Madrid, Spain

María A. Laguna-Marco, Daniel Haskel, and N. Souza-Neto
Advanced Photon Source, Argonne National Laboratory, Argonne, Illinois 60439, USA

Ronald I. Smith and William G. Marshall
ISIS Facility, RAL, Chilton, Didcot, Oxon OX11 0QX, United Kingdom

Gaston Garbarino and Mohamed Mezouar
European Synchrotron Radiation Facility (ESRF), BP 220, 6 rue Jules Horowitz, 38043 Grenoble Cedex, France

Alejandro Fernández-Martínez
LGIT, Université Grenoble and CNRS, M. Geosciences, BP 53, 38041 Grenoble, France and Institut Laue-Langevin, BP 156, 6 rue Jules Horowitz, 38042 Grenoble, France

Jesús Chaboy
Instituto de Ciencia de Materiales de Aragón, CSIC-Universidad de Zaragoza, 50009 Zaragoza, Spain

L. Fernandez Barquín
CITIMAC, Facultad de Ciencias, Universidad de Cantabria, 39005 Santander, Spain

J. A. Rodríguez Castrillón, M. Moldovan, and J. I. García Alonso
Department of Physical and Analytical Chemistry, University of Oviedo, Julián Clavería 8, Oviedo 33006, Spain

Jianzhong Zhang and Anna Llobet
Lujan Center for Neutron Scattering, LANL, Los Alamos, New Mexico 87545, USA

J. S. Jiang
Materials Science Division, Argonne National Laboratory, Argonne, Illinois 60439, USA
 (Received 23 July 2009; published 26 August 2009)

We have succeeded in increasing up to 150 K the Curie temperature in the Fe₆₄Ni₃₆ invar alloy by means of a severe mechanical treatment followed by a heating up to 1073 K. The invar behavior is still present as revealed by the combination of magnetic measurements with neutron and x-ray techniques under extreme conditions, such as high temperature and high pressure. The proposed explanation is based in a selective induced microstrain around the Fe atoms, which causes a slight increase in the Fe-Fe interatomic distances, thus reinforcing ferromagnetic interactions due to the strong magnetoelastic coupling in these invar compounds.

DOI: [10.1103/PhysRevB.80.064421](https://doi.org/10.1103/PhysRevB.80.064421)

PACS number(s): 75.50.Bb, 75.30.Kz

I. INTRODUCTION

It has been widely recognized that magnetism and structure are strongly interconnected.¹ In fact, it is well known that upon a marginal increase of the crystalline lattice parameter the magnetic exchange coupling is enhanced and probably the ferromagnetism is stabilized.^{2,3} Recently we have succeeded in synthesizing metastable FeCu alloys where at high temperatures the existence of γ -Fe precipitates, already proposed by Hernando *et al.* in the 90s,^{4,5} seems to be responsible for the appearance of ferromagnetism upon a small increase of the lattice constant that causes thermally induced low-spin (LS) to high-spin (HS) transitions.^{3,6-8} On the other

hand, the origin of the Invar effect, whereby these materials exhibit a low or near zero thermal expansion (LTE) coefficients below the magnetic ordering temperature has remained an issue of controversial debate for a long time.⁹⁻¹⁵ A microscopic explanation of the Invar effect in iron-nickel alloys has been given considering that the magnetic structure is characterized by a continuous transition from the ferromagnetic state at high volumes to a disordered noncollinear arrangement at low volumes.¹⁰

In simple words, there must be a negative contribution to the thermal expansion, which is related to the magnetic ordering, and which cancels out the ever-present positive contribution coming from the anharmonicity of the lattice

vibrations.^{3,16} Therefore, this effective temperature invariant thermal expansion can be exploited in a number of technological applications such as precision measurements for standards, large size cryogenic liquid containers, etc.^{15,17} Furthermore, the Invar effect is not limited to being a property of only Fe-Ni alloys, but it is also found in many other crystalline three dimensional (3D) systems such as Fe-Pt, Pd₃Fe, Fe₃C, or Fe-Cu,^{18–22} amorphous Fe alloys,^{23–25} as well as intermetallic systems such as R-Fe (R=Rare Earth).^{26,27} Hence, these alloys can be structurally ordered or disordered, ferromagnetic or antiferromagnetic. However, the thermal expansion coefficient is not the only physical property showing this anomalous Invar fingerprint,^{3,9,18,28} other physical properties (atomic volume, magnetic moment, bulk modulus or T_C) measured as a function of magnetic field, temperature or pressure also show striking behaviors.^{29–32} It has been observed the interdependence of the latter two variables in Ni-rich Fe-Ni compositions, where LS noncollinear magnetic ordering can be induced under pressure, giving rise to invar behavior.³³

In a previous work, we shown that the magnitude of the Curie temperature, T_C , of an standard commercial Fe₆₄Ni₃₆ powder sample can be increased in $\Delta T_C \sim 70$ K, by means of a severe mechanical processing, using a high-energy ball mill, followed by a heating up to 1073 K, while the invar character is maintained and its temperature range enlarged as well.³⁴ Previously, Dumpich *et al.*³⁵ already observed in “as-prepared” Fe₆₅Ni₃₅ evaporated thin films an increase in the T_C value of ca 200 K, accompanied by an enhancement of 20% in the saturation magnetization, M_s . However, both T_C and M_s drop down to the corresponding bulk values after annealing of the thin films. In spite of this, we will show that ΔT_C can be increased up to ~ 150 K in Fe₆₄Ni₃₆ invar material through the adequate variation of the milling conditions, being such enlarged value of T_C stable under subsequent heating-cooling procedures between RT and 1073 K.

We report here on a detailed study of the temperature and pressure dependencies of the crystalline lattice parameter, the magnetization and the x-ray magnetic circular dichroism in two Fe₆₄Ni₃₆ powders, the starting commercial (Standard Fe₆₄Ni₃₆) and the mechanical stressed (MS Fe₆₄Ni₃₆) ones, showing such outstanding finding. The stress-induced microstructural changes must play a definite role on the magnetic properties of these alloys. Thus, Invar FeNi materials show the extraordinary feature of enhancing the ordering temperature when they are mechanically stressed via high-energy ball milling. These LTE materials have the potential to reduce (or even eliminate) the effects of strain on material components in systems subjected to large temperature variations.

II. EXPERIMENTAL DETAILS

The starting Fe₆₄Ni₃₆ powder material was milled for 30 h in a high-energy planetary ball mill (Retsch PM/400) under controlled Ar atmosphere. The chemical composition of both standard and MS samples, Fe_{63.8(3)}Ni_{36.2(3)} and Fe_{63.4(2)}Ni_{36.6(2)}, respectively, was estimated by means of inductively coupled plasma mass spectroscopy using isotope

analysis. This information is very important to rule out a change of stoichiometry in the MS sample. The magnetic measurements were carried out using Faraday, SQUID, and PPMS (with VSM option) magnetometers. The magnetization vs. temperature curves, $M(T)$, were measured under two different values for the applied magnetic field, $H=300$ Oe and 6 kOe, in the temperature range between 4 K and 750 K. The magnetic field dependence of the magnetization, $M(H)$ curves, were measured at 5 K and 300 K under applied magnetic fields up to $H=90$ kOe. Neutron powder diffraction patterns were collected every 60 s from the two samples, in two successive controlled heating-cooling cycles from RT to 1073 K and back to RT again at 5 K/min, on the POLARIS time-of-flight diffractometer (ISIS facility, U.K.). Data collected over the time-of-flight range ~ 2000 – 19600 μ s in the backscattering detector bank, $\langle 2\theta \rangle = 145^\circ$, (corresponding to a d -spacing range of ~ 0.3 to 3.2 Å, which allowed more than 30 reflections from the fcc phase to be monitored) were analyzed by full-profile Rietveld refinement³⁶ using the FULLPROF suite package.³⁷ The wide d -spacing range allowed us to determine lattice parameters of both samples with accuracy better than 0.001 Å. Neutron powder diffraction experiments under high pressure were performed on PEARL (Rutherford Appleton Laboratory, U.K.) and HIPPO (Lujan Center for Neutron Scattering, LANL, USA) time-of-flight neutron diffractometers, in addition, x-ray diffraction (XRD) patterns under high pressure were collected on the beam line ID27 (ESRF, France). The x-ray magnetic circular dichroism (XMCD) experiments were separately performed in transmission geometry under high-pressure on the beam line 4ID-D-XOR at the Advanced Photon Source (ANL, USA).

III. RESULTS AND DISCUSSION

The diffraction patterns of both samples show the presence of reflections attributed, via a Rietveld refinement, to a single phase with a face-centered cubic (fcc) crystal structure (see Fig. 1). It is worthwhile to note that the lattice parameters, a , of the MS powders are systematically larger (0.1%) than those of the standard powders at room temperature (RT). This fact has been already observed in the case of milled powders of several binary intermetallic compounds, and is attributed to different causes.^{38–40} For the case reported here, it will be shown below that this increment of the lattice parameter at room temperature is due to the increase of the Curie temperature in an Invar material. Generally, in itinerant systems, expansion of the lattice parameter causes a decrease in the bandwidth, i.e., an increase in the density of states at the Fermi surface. As the result ferromagnetism becomes stable.

In Fig. 2, the $M(T)$ curve for the standard Fe₆₄Ni₃₆ alloy (red curve), measured under an applied magnetic field of $H=6$ kOe, is depicted showing a ferromagnetic (FM) behavior. The estimated Curie temperature is around 500 ± 10 K, in good agreement with earlier results in the literature.⁴¹ The $M(T)$ curve for the MS Fe₆₄Ni₃₆ sample exhibits a large enhancement in the value of T_C , (up to 650 ± 10 K). These findings can be understood on the basis of the magnetic coupling after milling between the MS crystals and the grain

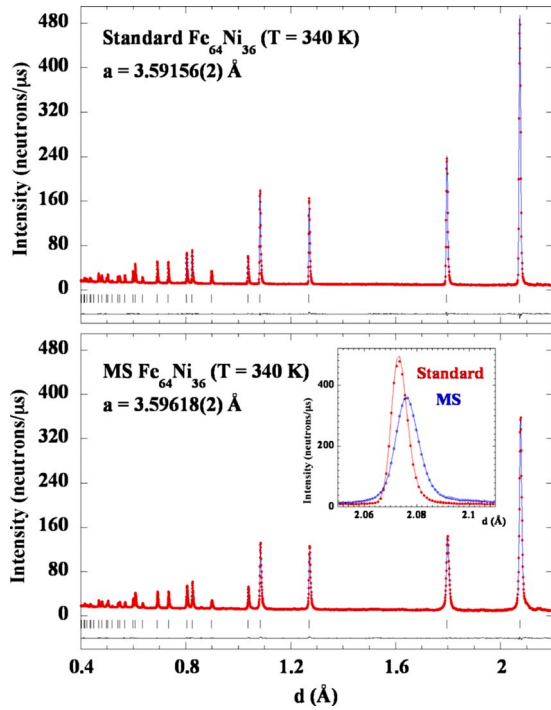


FIG. 1. (Color online) Fitted powder neutron diffraction patterns for standard (upper panel) and MS (lower panel) $\text{Fe}_{64}\text{Ni}_{36}$ samples. Observed (+) and calculated (solid line) patterns; positions of the Bragg reflections are represented by vertical bars. The observed-calculated difference is displayed at the bottom of each panel. The inset is a magnification of the (111) reflection.

boundaries that can induce variations in the intrinsic properties such as Curie temperature and/or magnetic anisotropy.^{42,43} Further heating-cooling cycles overlap the $M(T)$ curve of the treated sample even when the sample is measured again with time intervals of several years, indicating that the magnetic behavior of the milled powders is maintained and is reversible after a first heating up to 1073 K is done. Moreover, a Curie-Weiss behavior has been found,

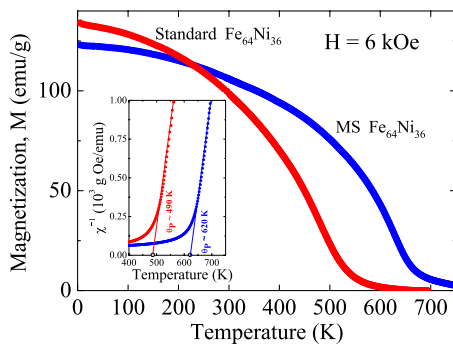


FIG. 2. (Color online) Magnetization vs temperature for the standard (red solid circles) and MS (blue solid circles) $\text{Fe}_{64}\text{Ni}_{36}$ samples measured under an applied magnetic field of 6 kOe. Note the increase in T_C from the standard sample to the MS one. Inset: Temperature dependence of the reciprocal magnetic susceptibility, χ^{-1} , showing a Curie-Weiss behavior near T_C . θ_p is the paramagnetic Curie temperature with values of 490 and 620 K for the standard and MS samples respectively.

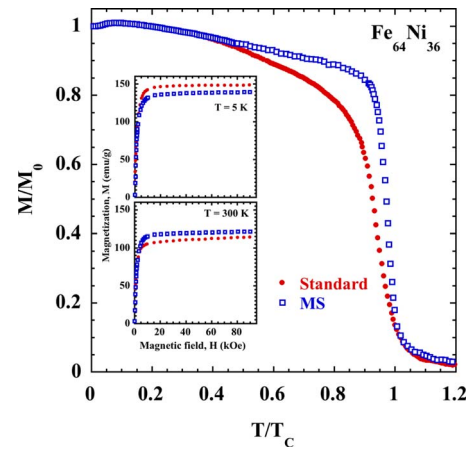


FIG. 3. (Color online) Normalized magnetization vs reduced temperature for the standard (red solid circles) and MS (blue open squares) $\text{Fe}_{64}\text{Ni}_{36}$ samples measured under an applied magnetic field of 300 Oe. The inset shows the $M(H)$ curves measured at $T=5$ and 300 K.

for both alloys, in the temperature dependence of the reciprocal magnetic susceptibility near T_C . The paramagnetic Curie temperatures, are $\theta_p \sim 490$ K and ~ 620 K, for standard and MS samples, respectively.

It is worth noting that $M(T)$ curves under low magnetic fields ($H \approx 300$ Oe) are quite different as it can be observed in Fig. 3, where the magnetization normalized to its value at $T=5$ K vs the reduced temperature, T/T_C , is shown in order to better appreciate the different behaviors for both samples. Both curves exhibit almost overlapping trends for temperatures $T < 0.4 T_C$ and $T > T_C$. However, the slope of the $M(T)$ curve is much higher (more negative) for the MS sample in the immediacy of the Curie point, suggesting a sharper transition into the paramagnetic state. Moreover, we show the $M(H)$ curves measured at $T=5$ K and 300 K (see inset in Fig. 3), where a slightly lower magnetization (less than 10%) is observed in the MS sample at low temperature (see also Fig. 2) probably due to frustration of Fe magnetic moments at the disordered grain boundaries.^{42,43}

The results plotted in Fig. 2 obviously suggest the need to carry out a detailed study of possible correlations between the crystal structures, the large increase in T_C , and the role played by magnetovolume effects. Specifically, it is of fundamental importance to determine whether this large enhancement of the Curie temperature also affects the thermal dependence of the expansion coefficient, α_T . If the material is found to exhibit Invar behavior with low values for α_T up to temperatures close to T_C , the temperature range for controlled thermal expansion will have been enlarged by more than 100 K, which would be of great interest for technological applications. It is a remarkable observation that for a non-Invar $\text{Fe}_{50}\text{Ni}_{50}$ alloy (the magnetovolume coupling in this material is much less important than in the standard Invar $\text{Fe}_{64}\text{Ni}_{36}$ one) the same physical treatment quoted above leads to a ΔT_C of less than 20 K instead of the 150 K found for the Invar composition.

From the analysis of the neutron diffraction patterns, the fcc lattice parameters at 340 K are $a=3.592(1)$ Å and

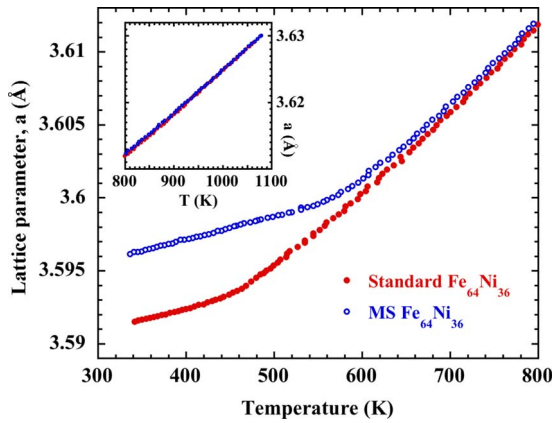


FIG. 4. (Color online) Temperature dependence of the fcc cubic lattice parameter, a , derived from time-of-flight powder neutron diffraction measurements, for standard (red solid circles) and MS (blue solid circles) $\text{Fe}_{64}\text{Ni}_{36}$ samples. The inset shows the high temperature dependence of the lattice parameter for both samples.

3.596(1) Å respectively, in good agreement with x-ray diffraction results (3.59187(1) Å and 3.59498(3) Å, respectively), indicating a relative volume increase of $\Delta V/V \approx 0.3\%$. It is important to note that the fcc structure remains unchanged over the whole temperature range of measurements for both samples,⁴⁴ although the lattice parameter value has increased (see above) and a slight peak broadening [see inset in Fig. 1, where the most intense reflection (111) is shown] is observed in the MS sample,³⁴ thus suggesting that internal microstrain is retained in the sample³⁶ after the mechanical and heat treatments.

The temperature dependence of the lattice parameters (see Fig. 4) for the two $\text{Fe}_{64}\text{Ni}_{36}$ materials (the standard and the MS samples) clearly shows the Invar character of both materials: above T_C the variation of the lattice parameter against temperature becomes linear, leading to a value for the thermal expansion coefficient, $\alpha_T \approx (17 \pm 1) \times 10^{-6} \text{ K}^{-1}$, typically expected for a normal metal. However, a drastic change of slope takes place below T_C , leading to a decrease in the value of α_T below $(3 \pm 1) \times 10^{-6} \text{ K}^{-1}$. The 450–550 K region where the changes in slope are observed due to the occurrence of magnetic ordering, is much higher than $\theta_D/2$ (in these FeNi materials the Debye temperature is $\theta_D \sim 370 \text{ K}$); i.e., the samples are well in the high temperature limit and zero point motion effects in thermal expansion coefficient are not important.

Two important differences between as received and treated samples can be immediately distinguished in Fig. 4: (i) the change of slope takes place, for the treated sample, at a temperature more than 100 K above that of the as received sample, thus confirming the correlation between the increase in the LTE temperature range and the raising of T_C ; and (ii) the lattice parameter grows 0.1% after milling and annealing, but only for temperatures below T_C . As can be observed the lattice parameters are practically identical for temperatures corresponding to the paramagnetic phase. This fact confirms that the increase in a observed below T_C after milling and heat treatment is a consequence of the enhancement of T_C .

In order to complete the characterization of the Invar behavior of these standard and MS samples, we, therefore, ex-

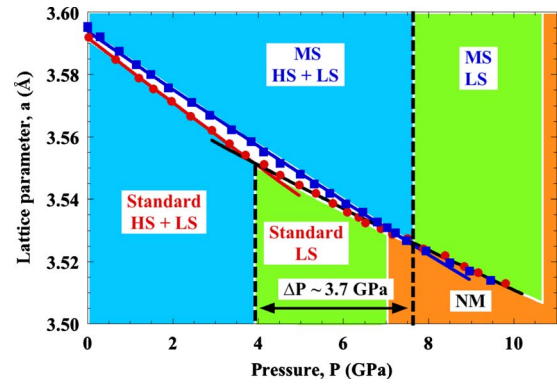


FIG. 5. (Color online) Pressure dependence of the lattice parameter for standard (red solid circles) and MS (blue solid squares) $\text{Fe}_{64}\text{Ni}_{36}$ samples measured at room temperature. The solid lines correspond to a fit to a first-order Murnaghan equation of state for the mixture of the HS+LS states and the pure LS state. The HS+LS, LS, and NM regions are shaded in light blue, light green and orange colors (see text for more details).

amine the pressure dependence of the cell parameter and the Curie temperature. In particular, studies of magnetization under high pressure are far from common. It is well known that there are obvious difficulties in combining the requirements of high-pressure technology and classical magnetometry.^{30,32,45}

In Fig. 5, we compare the pressure dependence of the cell parameter for fcc standard and MS samples at RT, showing a change of slope around 3.9 GPa (in good agreement with other recent works^{33,46,47}) and 7.6 GPa, respectively. The fcc lattice remains stable without any crystalline structural transformation over the whole pressure range up to 10 GPa. The dependencies of the cell parameter of both samples converge around 8 GPa and exhibit a similar pressure dependence above this pressure, while they clearly diverge below 8 GPa indicating that the standard and the MS samples have a different HS+LS ground state. In fact, these dependencies have been well fitted to a first-order Murnaghan equation of state⁴⁸ considering the values of the Bulk modulus, B , as a fitting parameter and that of $\frac{dB}{dP}$ has been set to the value of 1.42 and 3.6 for the HS+LS and LS states, respectively, obtained from ultrasonic measurements.²⁹ The best refinement leads to the values of B around 113 GPa and 127 GPa for standard and MS samples, respectively, at RT and atmospheric pressure, i.e., the compressibility of the standard sample is larger than that of the MS one. This fact could be understood taking into account that (i) the mechanically stressed sample is probably filled with dislocations and defects after milling that interfere so strongly with each other that the compressibility is found to drop significantly; and (ii) the HS+LS states of both materials could be different by the effects of irreversible strain induced during the milling process performed at room temperature, which is below the Curie temperature of the $\text{Fe}_{64}\text{Ni}_{36}$ standard Invar alloy.

Figure 6 displays the pressure dependence of the peak-to-peak XMCD magnitude for standard and MS samples measured at the Fe K -edge and collected at RT. The XMCD spectra of the standard sample are similar to those measured in the FeNi alloys.⁴⁹ The lower XMCD signal for the stan-

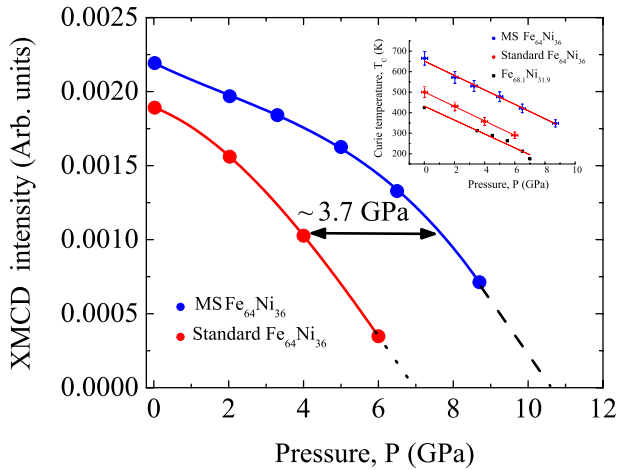


FIG. 6. (Color online) Pressure dependence of the peak-to-peak XMCD signal at the Fe K-edge for standard (red solid circles) and MS (blue solid circles) Fe₆₄Ni₃₆ samples measured at room temperature. The solid line is a guide for the eyes. The inset shows the pressure dependence of the Curie temperature of both materials (see text for more details). The data of the Fe_{68.1}Ni_{31.9} Invar alloy are taken from the reference.⁴⁵

standard sample at ambient pressure agrees with the magnetization results in Figs. 2 and 3 ($T=300$ K). Increasing pressure both XMCD signals start to decrease with a moderate rate at the pressures where the respective cell parameters of these materials showed a change of slope (see Fig. 5). At high pressure we observe a tendency to collapse, in a similar way to that reported for cementite (Fe₃C).²¹ It is important to determine whether this XMCD collapse is due to the expected transition from a LS state to a nonmagnetic one or due to a concomitant decrease in Curie temperature. Assuming that the $M(T)$ dependence of Fig. 2 is universal under pressure, we have been able to estimate the dependence of T_C with pressure using the XMCD values for each pressure. The inset of Fig. 6 shows that these dependencies are fairly linear ($-\frac{dT_C}{dP} \approx 35$ K/GPa for both materials) and similar to that of the Invar Fe_{68.1}Ni_{31.9} ($-\frac{dT_C}{dP} = 33$ K/GPa).⁴⁴ In the same way, an estimation of $-\frac{dT_C}{dP}$ can be also obtained from both the neutron diffraction under pressure and magnetization results (see Figs. 2 and 5). From these it seems that 3.7 GPa corresponds to 150 K; so $-\frac{dT_C}{dP} \approx 40$ K/GPa, which is quite close to the value determined above from XMCD. Extrapolating the XMCD magnitude to zero value at room temperature (measured at around 300 K), which makes that the transition temperature to a nonmagnetic state drops to 300 K in both materials, we obtain critical pressures of ~ 7.0 GPa and ~ 10.7 GPa, for Fe₆₄Ni₃₆ standard and MS samples, respectively. The difference 3.7 GPa in the values of these critical pressures is in quite good agreement with the difference found in the values of pressure where the change of slope in the cell parameters takes place (see Fig. 5). Furthermore, extrapolating to zero the value of T_C from the $T_C(P)$ variation (see the inset of Fig. 6) leads to the values of ~ 13 GPa and ~ 17 GPa for the pressures needed in order to stabilize the NM state in standard and MS Fe₆₄Ni₃₆ samples, respectively. These critical pressures correspond to the val-

ues of the magnetic phase transition from the LS to the nonmagnetic state obtained by inelastic x-ray scattering.⁵⁰

As a consequence, it seems that in addition to the fact that the treated Fe-Ni Invar alloy become harder to squeeze under pressure, we need to add the feature that owing to the important magnetoelastic coupling in these materials, when they are mechanically stressed below T_C , these systems increase notoriously their Curie temperature, leading to an enhancement of the Invar properties, where an almost zero thermal expansion is observed. Up to now the usual way to attempt to increase T_C in this FeNi system is through increasing the Ni content, however, in doing so the magnetovolume effects lose importance because Ni atoms stabilize much more the HS state. Ball milling followed by high temperature annealing overcomes these shortcomings. Moreover, x-ray absorption experiments in both Fe-K and Ni-K edges revealed a more disordered local environment around the Fe atoms,³⁴ suggesting that mechanical stressing of the invar powders mostly affects the Fe-Fe interatomic distances because a slight increase of such distances favors ferromagnetism.

IV. CONCLUSIONS

In summary, the mechanically stressed and thermally treated Fe₆₄Ni₃₆ alloy exhibits an outstanding enhancement of an intrinsic physical property such as the Curie temperature, being the LTE range extended as well. Up to now, the research effort in Invar materials with larger LTE temperature ranges has been mainly focused on the search for new compositions instead of changing the microstructure with the aim of varying the magnetovolume coupling. Furthermore, this work opens new horizons and directions significantly different from those currently being pursued in the so-called Invar problem, which during the last century was mostly oriented in understanding the mechanism leading to LTE. In particular, other deeply mysterious issues about which we have very little comprehension is the enhancement of an intrinsic property, such as the Curie magnetic ordering temperature, in this new modified Invar Fe₆₄Ni₃₆ alloy, will also deserve much more interest and effort within the scientific community.

ACKNOWLEDGMENTS

We thank ISIS, Lujan Neutron Scattering Center at LANL-SCE, APS and ESRF for the allocation of neutron and synchrotron beam time, and the SCT at the University of Oviedo for the high-resolution XRD facility. This work was partially supported by FEDER and the Spanish MICINN (Grant No. MAT2008-06542-C04). M.A.L-M acknowledges MICINN for Postdoctoral grant. Work at Argonne & Los Alamos National Laboratories was supported by the U.S. Department of Energy, Office of Science, under Contracts No. DE-AC02-06CH11357 and No. DE-AC52-06NA25396, respectively.

- ¹A. Aharoni, *Introduction to the Theory of Ferromagnetism* (Clarendon Press, Oxford, 1996).
- ²P. W. Anderson, *Phys. Rev.* **124**, 41 (1961).
- ³W. Pepperhoff and M. Acet, *Constitution and Magnetism of Iron and its Alloys* (Springer, Berlin, 2001).
- ⁴A. Hernando, P. Crespo, J. M. Barandiarán, A. García Escorial, and R. Yavari, *J. Magn. Magn. Mater.* **124**, 5 (1993).
- ⁵A. Hernando, P. Crespo, A. García-Escorial, and J. M. Barandiarán, *Phys. Rev. Lett.* **70**, 3521 (1993).
- ⁶P. Gorria, D. Martínez-Blanco, J. A. Blanco, M. J. Pérez, A. Hernando, L. Fernández Barquín, and R. I. Smith, *Phys. Rev. B* **72**, 014401 (2005).
- ⁷S. L. Palacios, R. Iglesias, D. Martínez-Blanco, P. Gorria, M. J. Pérez, J. A. Blanco, A. Hernando, and K. Schwarz, *Phys. Rev. B* **72**, 172401 (2005).
- ⁸P. Gorria, D. Martínez-Blanco, R. Iglesias, S. L. Palacios, M. J. Pérez, J. A. Blanco, L. Fernández Barquín, A. Hernando, and M. A. González, *J. Magn. Magn. Mater.* **300**, 229 (2006).
- ⁹E. F. Wassermann, in *Ferromagnetic Materials*, edited by K. H. J. Buschow and E. P. Wohlfarth (North-Holland, Amsterdam, 1990), Vol. 5, p. 237.
- ¹⁰M. van Schilfgaarde, I. A. Abrikosov, and B. Johansson, *Nature (London)* **400**, 46 (1999).
- ¹¹V. Crisan, P. Entel, H. Ebert, H. Akai, D. D. Johnson, and J. B. Staunton, *Phys. Rev. B* **66**, 014416 (2002).
- ¹²A. V. Ruban, S. Khmelevskiy, P. Mohn, and B. Johansson, *Phys. Rev. B* **76**, 014420 (2007).
- ¹³I. A. Abrikosov, A. E. Kissavos, F. Liot, B. Alling, S. I. Simak, O. Peil, and A. V. Ruban, *Phys. Rev. B* **76**, 014434 (2007).
- ¹⁴Y. Tsunoda, L. Hao, S. Shimomura, F. Ye, J. L. Robertson, and J. Fernandez-Baca, *Phys. Rev. B* **78**, 094105 (2008).
- ¹⁵Y. Nakamura, *IEEE Trans. Magn.* **12**, 278 (1976).
- ¹⁶M. Acet, H. Zähres, E. F. Wassermann, and W. Pepperhoff, *Phys. Rev. B* **49**, 6012 (1994).
- ¹⁷P. Mohn, *Nature (London)* **400**, 18 (1999).
- ¹⁸E. F. Wassermann, *J. Magn. Magn. Mater.* **100**, 346 (1991).
- ¹⁹B. Rellinghaus, J. Kästner, T. Schneider, E. F. Wassermann, and P. Mohn, *Phys. Rev. B* **51**, 2983 (1995).
- ²⁰P. Gorria, D. Martínez-Blanco, J. A. Blanco, A. Hernando, J. S. Garitaonandia, L. Fernández Barquín, J. Campo, and R. I. Smith, *Phys. Rev. B* **69**, 214421 (2004).
- ²¹E. Duman, M. Acet, E. F. Wassermann, J. P. Itié, F. Baudelet, O. Mathon, and S. Pascarelli, *Phys. Rev. Lett.* **94**, 075502 (2005).
- ²²M. L. Winterrose, M. S. Lucas, A. F. Yue, I. Halevy, L. Mauger, J. A. Muñoz, Jingzhu Hu, M. Lerche, and B. Fultz, *Phys. Rev. Lett.* **102**, 237202 (2009).
- ²³J. A. Fernández-Baca, J. W. Lynn, J. J. Rhyne, and G. E. Fish, *Phys. Rev. B* **36**, 8497 (1987).
- ²⁴J. M. Barandiarán, P. Gorria, I. Orúe, M. L. Fdez-Gubieda, F. Plazaola, and A. Hernando, *Phys. Rev. B* **54**, 3026 (1996).
- ²⁵P. Gorria, J. S. Garitaonandia, M. J. Pérez, J. A. Blanco, and J. Campo, *Phys. Status Solidi (RRL)* **3**, 28 (2009).
- ²⁶D. Givord and R. Lemaire, *IEEE Trans. Magn.* **10**, 109 (1974).
- ²⁷P. Gorria, P. Álvarez, J. Sánchez Marcos, J. L. Sánchez Llamazares, M. J. Pérez, and J. A. Blanco, *Acta Mater.* **57**, 1724 (2009).
- ²⁸G. Hausch and H. Warlimont, *Acta Metall.* **21**, 401 (1973).
- ²⁹F. Decremps and L. Nataf, *Phys. Rev. Lett.* **92**, 157204 (2004).
- ³⁰M. Matsushita, Y. Miyoshi, S. Endo, and F. Ono, *Phys. Rev. B* **72**, 214404 (2005).
- ³¹M. Matsushita, T. Inoue, I. Yoshimi, T. Kawamura, Y. Kono, T. Irifune, T. Kikegawa, and F. Ono, *Phys. Rev. B* **77**, 064429 (2008).
- ³²M. Matsushita, H. Ogiyama, and F. Ono, *J. Magn. Magn. Mater.* **321**, 595 (2009).
- ³³L. Dubrovinsky, N. Dubrovinskaia, I. A. Abrikosov, M. Vennström, F. Westman, S. Carlson, M. van Schilfgaarde, and B. Johansson, *Phys. Rev. Lett.* **86**, 4851 (2001).
- ³⁴P. Gorria, R. Boada, A. Fernández-Martínez, G. Garbarino, R. I. Smith, J. Chaboy, J. I. García Alonso, D. Martínez-Blanco, G. R. Castro, M. Mezouar, A. Hernando, and J. A. Blanco, *Phys. Status Solidi (RRL)* **3**, 115 (2009).
- ³⁵G. Dumpich, J. Kästner, U. Kirschbaum, H. Mühlbauer, J. Liang, Th. Lübeck, and E. F. Wassermann, *Phys. Rev. B* **46**, 9258 (1992).
- ³⁶D. Martínez-Blanco, P. Gorria, J. A. Blanco, M. J. Pérez, and J. Campo, *J. Phys.: Condens. Matter* **20**, 335213 (2008).
- ³⁷J. Rodríguez-Carvajal, *Physica B* **192**, 55 (1993).
- ³⁸H. Bakker, G. F. Zhou, and H. Yang, *Prog. Mater. Sci.* **39**, 159 (1995).
- ³⁹C. Suryanarayana, *Prog. Mater. Sci.* **46**, 1 (2001).
- ⁴⁰P. Gorria, D. Martínez-Blanco, M. J. Pérez, J. A. Blanco, and R. I. Smith, *J. Magn. Magn. Mater.* **294**, 159 (2005).
- ⁴¹J. Crangle and G. C. Hallam, *Proc. R. Soc. Lond. A* **272**, 119 (1963).
- ⁴²A. Hernando, I. Navarro, and P. Gorria, *Phys. Rev. B* **51**, 3281 (1995).
- ⁴³J. S. Garitaonandia, P. Gorria, L. Fernández Barquín, and J. M. Barandiarán, *Phys. Rev. B* **61**, 6150 (2000).
- ⁴⁴C. Kuhrt and L. Schultz, *J. Appl. Phys.* **73**, 1975 (1993).
- ⁴⁵M. Matsushita, S. Endo, K. Miura, and F. Ono, *J. Magn. Magn. Mater.* **265**, 352 (2003).
- ⁴⁶L. Nataf, F. Decremps, M. Gauthier, and B. Canny, *Phys. Rev. B* **74**, 184422 (2006).
- ⁴⁷L. Nataf, F. Decremps, M. Gauthier, and G. Syfosse, *Ultrasonics* **44**, e555 (2006).
- ⁴⁸F. D. Murnaghan, *Proc. Natl. Acad. Sci. U.S.A.* **30**, 244 (1944).
- ⁴⁹H. Sakurai, F. Ito, H. Maruyama, A. Koizumi, K. Kobayashi, H. Yamazaki, Y. Tanji, and H. Kawata, *J. Phys. Soc. Jpn.* **62**, 459 (1993).
- ⁵⁰J. P. Rueff, A. Shukla, A. Kaprolat, M. Krisch, M. Lorenzen, F. Sette, and R. Verbeni, *Phys. Rev. B* **63**, 132409 (2001).